

The High Temperature Behavior of Superalloys Exposed to Sodium Chloride: II. Corrosion

F. MANSFELD, N. E. PATON, AND W. M. ROBERTSON

The corrosion behavior of various superalloys in molten NaCl has been examined by weight loss measurements, analysis of corrosion products, and potentiostatic polarization curves. Corrosion rates were higher in platinum than in quartz crucibles, relatively independent of alloy composition, but highly dependent on oxygen pressure. The high corrosion rates and the shape of the polarization curves indicate that the oxides formed in molten NaCl are not protective. Analysis of the sodium content in the alloy after exposure to molten NaCl indicates diffusion of sodium into the bulk of the metal. The effect of oxygen and the higher corrosion rates in platinum crucibles are explained by thermodynamic and kinetic considerations.

IN the preceding paper,¹ the effect of high temperature exposure to NaCl on the mechanical properties of superalloys (Inconel 718, Inconel 625, Rene' 41, Haynes 188, TD-NiCr) has been studied. Residual mechanical properties, as determined by a postexposure tensile test, were found to be seriously degraded, the amount of degradation being dependent on the partial pressure of oxygen in the environment. Creep rates were increased up to three orders of magnitude in the presence of NaCl at temperatures around 1000°C.

In order to obtain information regarding corrosion rates of the various superalloys, the composition of corrosion products, and the effect of oxygen, experiments were also carried out in molten NaCl. Results of these investigations are reported in this communication. In molten NaCl, it is possible to study the electrochemical behavior of alloys by recording polarization curves, as has been done with great success in aqueous media. These electrochemical techniques have recently been employed by Rahmel² in a study of iron and several steels in a eutectic alkali sulfate melt, and by Baudo, Tamba, and Bombara³ in an electrochemical investigation of corrosion of ferritic steels in molten sulfates. Janz and Conte⁴ conducted potentiostatic polarization studies on stainless steel in fused carbonates, while Devyatkin and Ukshe⁵ studied the behavior of iron in molten chlorides. No electrochemical studies in molten salts have been reported previously for the alloys of interest in the present study.

In this investigation the corrosion rates of the alloys were determined from weight loss data, while the corrosion products were analyzed by mass spectroscopy, atomic absorption spectroscopy, and X-ray diffraction. Mass spectroscopy was also used to detect diffusion of sodium and chlorine into the bulk of the metals. Polarization curves have been obtained by potentiostatic measurements.

F. MANSFELD, N. E. PATON, and W. M. ROBERTSON are Members of the Technical Staff, North American Rockwell Science Center, Thousand Oaks, Calif. 91360.

Manuscript submitted March 13, 1972.

EXPERIMENTAL RESULTS

I) Weight Loss Data

MEASUREMENTS IN AIR

Weighed samples of superalloys about $1\frac{1}{4}$ by $\frac{3}{4}$ by 0.02 in. were placed in a quartz or platinum crucible which was then filled with NaCl and placed in a quartz tube. The tube was placed into a furnace at $820 \pm 10^\circ\text{C}$. After about 24 h, the crucible was taken out of the quartz tube, and after the melt had solidified, immersed in hot distilled water. The specimen was taken out of the resulting solution, dried and weighed again. Based on the time of the experiment, the recorded weight loss Δm and the area of the specimen, the corrosion rate r in mdd ($\text{mg}/\text{dm}^2 \text{ day}$) was calculated. Values are reported in Table I. These values might be somewhat too low, since in most cases not all of the corrosion products were removed from the surface by boiling in distilled water. In the case of Haynes 188 and Hastelloy N, where a dense layer of corrosion products formed on the surface, this layer was scraped off before weighing.

Experiments in a platinum crucible were carried out in order to study the effect of galvanic coupling of the specimen to a more noble metal. In the tests with Inconel 718, the effect of KCl was compared to that of NaCl; in order to get information concerning the role of oxygen in the corrosion process, one test was run in a nitrogen atmosphere.

A comparison of the data in Table I shows that the

Table I. Corrosion Rate r of Superalloys in Salt, 820°C , 24 h Test

Alloy	Environment	Quartz Crucible r , mdd	Pt Crucible r , mdd
Inco 718	NaCl, air	135	2980
Inco 718	KCl, air	—	2570
Inco 718	NaCl, N_2	—	1680
Rene' 41	NaCl, air	253	4760
Haynes 188	NaCl, air	805	6240
TD NiCr	NaCl, air	150	5940
Hastelloy N	NaCl, air	344	9300
Nickel	NaCl, air	349	511

corrosion rates of superalloys in molten NaCl, which are already high in a quartz crucible, are greatly increased when a platinum crucible is used, where the specimen is in contact with the platinum and a galvanic couple is established. Results show that corrosion rates are not very different in NaCl and KCl, whereas corrosion rates drop when the experiments are carried out in an inert atmosphere.

MEASUREMENTS IN VACUUM

In order to obtain more information concerning environmental effects, experiments were carried out in vacuum using NaCl as-received, or dried by melting and cooling under reduced pressure (about 70 μ).

In one set of experiments the test specimen was placed in a quartz tube, which was then filled with NaCl and sealed under vacuum. For Inconel 718, no weight loss was observed after the 24 h test at 820°C with the specimen immersed in dried NaCl, although a very thin layer of gray corrosion products covered the surface. A residual property test of this alloy showed a slight decrease in yield and ultimate tensile strength comparable to that for samples exposed in air for the same time and temperature in the absence of salt, but not the severe degradation of properties as reported in Ref. 1. In as-received NaCl, the specimen gained weight (about 0.4 mg/cm²) and was covered with a black-green deposit.

In a different kind of experiment, the specimen (Inconel 718) was placed in a platinum crucible in the quartz tube which was connected to a vacuum pump. The NaCl was molten under reduced pressure (about 70 μ). All NaCl evaporated from the crucible during this test and condensed at the cooler parts of the quartz tube. It is, therefore, not known how long the specimen was exposed to the melt. After the 24 h test at 820°C, no weight loss could be detected, although the specimen was covered with a thin layer of Cr₂O₃ as determined by X-ray analysis.

These results show that moisture in NaCl contributes to oxidation of the metal and corrosion. The corrosion rates are, however, drastically reduced in the absence of oxygen.

II) Analysis of Corrosion Products

After dissolution of the solidified melt in H₂O, the insoluble part of the corrosion products was separated from the soluble part and analyzed by mass spectroscopy. Results of this analysis, in weight percent, after eliminating Na, Cl, and O, are given in Table II. Values in parentheses give the bulk composition of the alloys (weight percent). The soluble part was analyzed by atomic absorption spectroscopy, Table III.

The solid corrosion products were also analyzed by X-ray diffraction. The following compounds were found for the different alloys:

Inco 718:	Cr ₂ O ₃ , Fe ₃ O ₄ or NiFe ₂ O ₄
Haynes 188:	CoWO ₄ , CoNiO ₂ , CoCr ₂ O ₄ and/or NiCr ₂ O ₄
Hastelloy N:	NiO, NiFe ₂ O ₄ , NiCr ₂ O ₄
TD NiCr:	NiO, Some Cr ₂ O ₃ , trace ThO ₂
Ni:	NiO

Table II. Spectroscopic Analysis of Solid Corrosion Products (Weight Percent), Experiments in Platinum Crucible. (Compositions of Alloys are Given in Parentheses)

	Inco 718	Rene' 41	Haynes 188	TD NiCr	Hastelloy N
Ni	5.3 (53)	35.0 (52)	21.0 (22)	82.9 (78)	82.3 (72)
Cr	55.7 (19)	25.1 (19)	12.1 (22)	8.9 (20)	8.2 (7.5)
Co	—	23.8 (11)	39.5 (40)	— (—)	0.3 (—)
Fe	27.9 (18)	4.6 (3)	1.1 (3)	— (—)	5.1 (4)
Mo	—	0.2 (10)	— (—)	— (—)	1.7 (16)
Ti	6.2 (0.8)	7.5 (3)	— (—)	— (—)	— (—)
Al	—	3.2 (1.5)	— (—)	— (—)	— (—)
Cb	4.6 (5.2)	— (—)	— (—)	— (—)	— (—)
W	— (—)	— (—)	23.8 (14)	0.4 (—)	— (—)
Th	— (—)	— (—)	— (—)	7.8 (2)	— (—)

Table III. Analysis of Soluble Corrosion Products. (Experiments in Platinum Crucible.)

a = Percent of Total Soluble Corrosion Products b = Percent of Total Weight Loss										
	Inco 718		René 41		Haynes 188		TDNiCr		Hastelloy N	
	a	b	a	b	a	b	a	b	a	b
Ni	84	2.8	52	5.8	21	0.4	99	1.9	93	3.2
Cr	~5	~0.2	3	0.4	<1	<0.1	~1	<0.1	<1	<0.1
Co	<2	<0.1	37	4.2	69	1.3	—	—	~1	<0.1
Fe	—	—	5	0.6	~4	<0.1	—	—	~2	<0.1
Mo	<4	<0.1	2	0.1	1	<0.1	—	—	~2	<0.1
Ti	<5	<0.2	—	—	<4	<0.1	—	—	<1	<0.1
Al	—	—	<1	<0.1	—	—	—	—	—	—

While stoichiometric oxides are listed here, it is very likely that the oxides formed as corrosion products contain other metals as impurities.

III) Sodium Diffusion

In order to study the possibility of sodium diffusion into the metal during hot salt corrosion, Rene' 41 and TD-NiCr were immersed in molten NaCl at 820°C for 24 h. The samples ($\frac{1}{4}$ by $\frac{1}{2}$ by 1 in.) were removed from the melt and washed in distilled water. After careful removal of corrosion products and NaCl from the melt and polishing, a new surface was exposed by spark cutting as indicated in Fig. 1 and analyzed by mass spectroscopy for sodium and chlorine in the area between the two arrows in Fig. 1 thereby avoiding edge effects. The data for Rene' 41 in Fig. 1 indicate an enrichment of Na over the average bulk concentration of about 165 ppm when the surface is approached. Since no similar increase of chlorine was observed and the chlorine concentration is always lower than the sodium concentration, it seems that sodium has diffused into the metal as opposed to penetration of molten NaCl into cracks and fissures. Similar results were obtained for TD-NiCr.

Samples of each alloy were examined metallographically after corrosion tests. For all alloys evidence of extensive grain boundary attack was detected, but most severe attack was found for Haynes 188, Fig. 2(a). Based on the corrosion rate reported in Table I for the specimen shown in Fig. 2(a) (6240 mdd), a reduction in thickness of 70 μ (2.8 mil) is calculated while about 90 μ (3.5 mil) were measured. This represents a uniform attack while Fig. 2(a) shows a further penetration

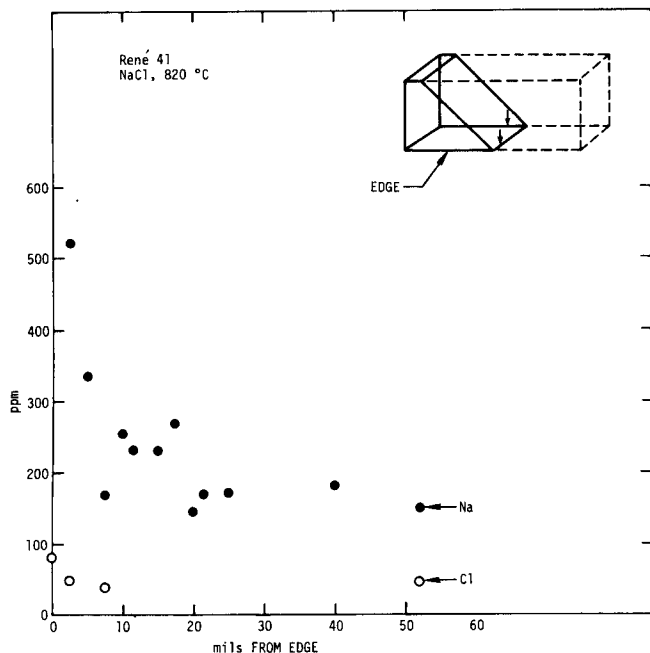


Fig. 1—Spectroscopic analysis of Rene' 41 for sodium and chlorine after immersion in NaCl at 820°C for 24 h.

of grain boundaries of about $100\ \mu$ (4 mil) after exposure to molten NaCl for 24 h. This indicates that the reduction of mechanical properties reported by the authors¹ is probably due to intergranular corrosion. Electron probe microanalysis of the Haynes 188 sample, Fig. 2(b), revealed considerable chromium loss in the grain boundaries as shown in Fig. 2(c). No sodium contamination was detected in the grain boundaries but the electrolytic method used for sample preparation might have leached sodium out of the surface to a depth sufficient to mask its presence in the microprobe analysis. Sodium may, therefore, have been present in the grain boundaries, but was not detected with the method employed.

IV) Potentiostatic Polarization Curves

In these experiments, the current flowing between the test specimen and a counter electrode is measured while a constant potential is applied between the test specimen and a reference electrode using a potentiostat. The platinum crucible was used as a counter electrode, while a silver wire immersed in a melt of NaCl-1 pct AgCl in a quartz tube was used as a reference electrode. The quartz tube containing the reference electrode has been described in more detail by Rahmel² based on earlier studies of Danner and Rey.⁶ This electrode was immersed in the molten salt without touching the platinum crucible or the test specimen. The test specimen, which was hanging on a platinum wire, which was sealed in a quartz tube, was totally immersed in the melt. This arrangement is schematically shown in Fig. 3. Electrical contact to the platinum crucible was made through a platinum wire. The quartz tube was closed by a cover which contained joints through which the quartz tube containing the reference electrode, the test electrode, and the wire to the platinum crucible could be introduced into the test cell. It also contained an inlet and an outlet for nitrogen.

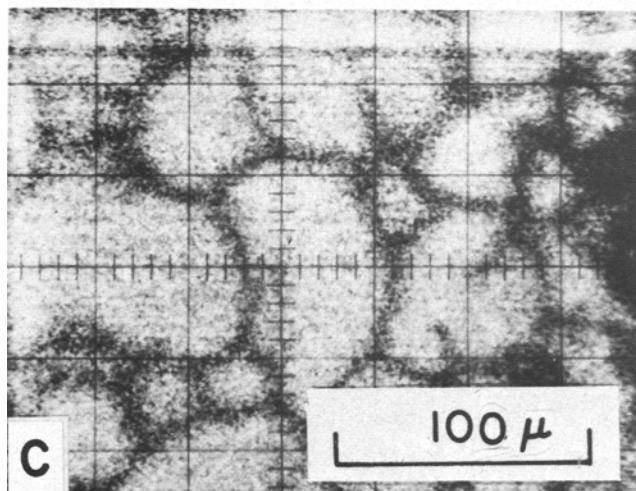
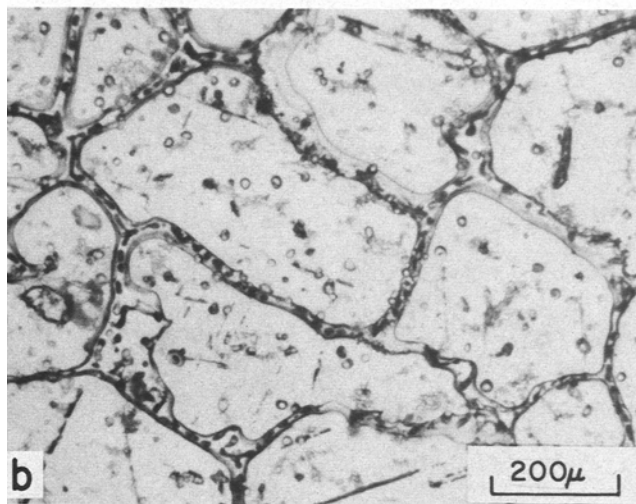
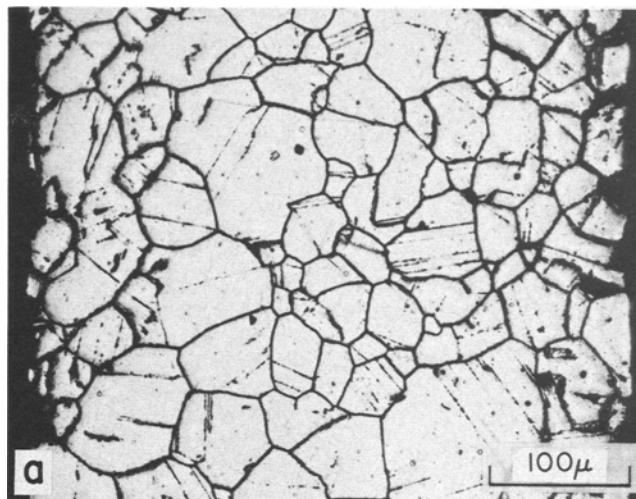


Fig. 2—Haynes 188 exposed at 982°C (1800°F) for 48 h in air with 0.015 inches NaCl on surface. (a) Cross section. (b) Optical micrograph. (c) CrK α X-ray image showing chromium depletion at grain boundaries.

Although only a limited number of polarization curves have been obtained, certain general conclusions can be drawn from these curves, of which Fig. 4 is an example. The oxides formed on the alloys while immersed in molten NaCl at $820 \pm 10^\circ\text{C}$ are not protective as indi-

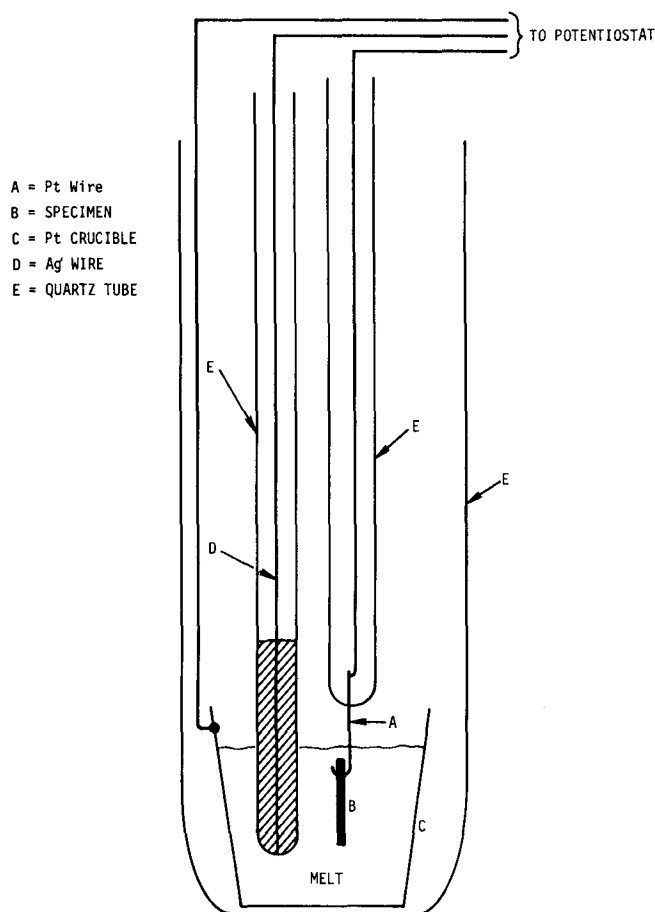


Fig. 3—Experimental arrangement for polarization studies.

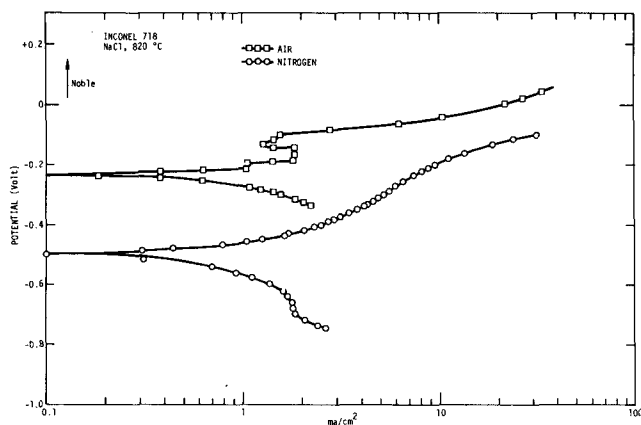


Fig. 4—Potentiostatic polarization curves for Inconel 718 in molten NaCl, 825°C.

cated by the lack of a passive region. There seems to be a small region of passivity when Inconel 718 (Fig. 4, experiment in air) and TD-NiCr are polarized into the noble direction. Apparently the passive film is destroyed, however, by localized attack in the form of pitting on further polarization. Microscopic observation of the surface of TD-NiCr after the polarization experiments showed indeed a number of hemispherical pits, Fig. 5. In the case of Rene' 41 some grains were completely removed; in addition, there seems to be severe intergranular attack, Fig. 6. The shift of the whole polarization curve in the less noble (active) di-

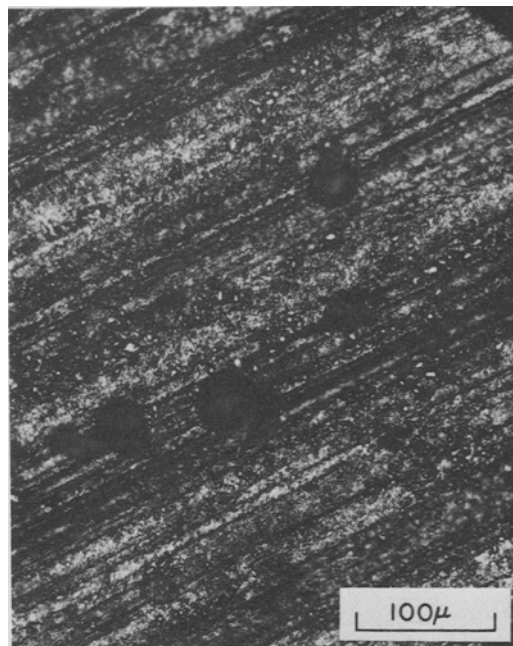


Fig. 5—Photomicrograph of TD Ni-Cr after potentiostatic polarization experiment in molten NaCl, 825°C.

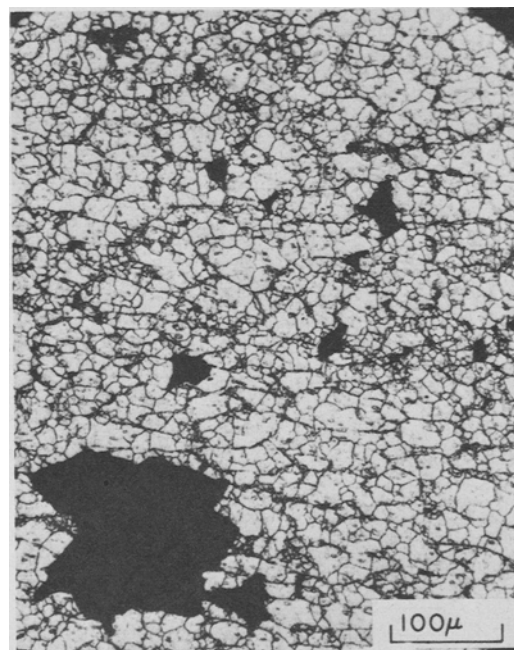


Fig. 6—Photomicrograph of Rene' 41 after potentiostatic polarization experiment in molten NaCl, 825°C.

rection when the experiment was conducted in a nitrogen atmosphere instead of air was observed for all metals studied.

For nickel no polarization curves were obtained. Metallographic observation of a specimen (sheet of 0.0075 in. thickness) from weight loss experiments in a quartz crucible, Table II, indicates, however, that pitting and strong intergranular corrosion occur even for an unpolarized specimen, Fig. 7. This form of localized attack led to perforation of the specimen at several locations.

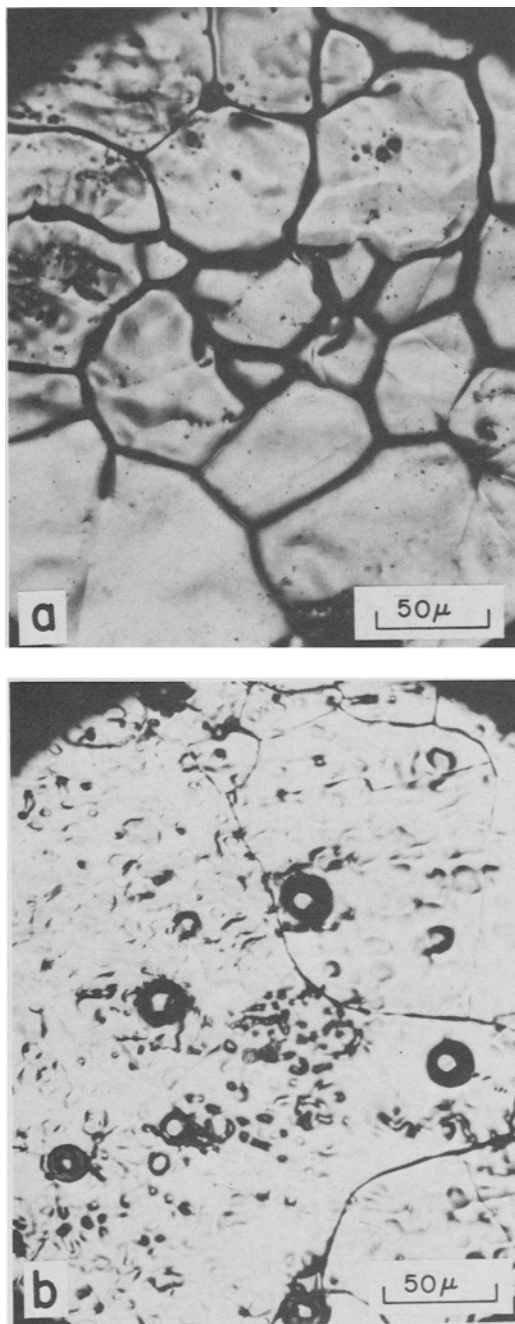


Fig. 7—Photomicrograph of nickel after immersion test in molten NaCl, 825°C, (a) Intergranular attack. (b) Pitting.

DISCUSSION

Effect of Oxygen and Water

The results of our corrosion studies in Table I have shown clearly that all alloys studied and pure nickel suffer severe corrosion when immersed in molten NaCl provided that oxygen is present. Similar results have been obtained by Moskowitz and Redmerski⁷ in a study of the corrosion behavior of superalloys in the presence of KCl or LiF between 870° and 1040°C. The detrimental effect of oxygen which was also observed in our studies of the mechanical properties of these alloys¹ can be seen from Table I when experiments with Inconel 718 in air are compared with those in a nitrogen atmosphere. The experiments in vacuum or under re-

duced pressure show even more drastically the damaging action of oxygen. A small effect of moisture contained in undried NaCl is also observed.

The effects of oxygen are to be expected from the thermodynamics of corrosion in fused chlorides and have been treated by Edeleanu and Littlewood.⁸ The effect of oxygen is related to the reversible potential of the melt ϕ_{rev} , which depends on the O_2/O^{2-} equilibrium:



in the form

$$\phi_{\text{rev}} = \phi_{\text{rev}}^0 + \frac{2.3RT}{2F} \log \frac{\sqrt{P_{\text{O}_2}}}{a_{\text{O}^{2-}}} \quad [2]$$

where ϕ_{rev}^0 is the equilibrium potential and R , T , and F have their usual meaning. Similar to the pH value in aqueous electrolytes, which is related to the activity a_{H^+} of the proton ($\text{pH} = -\log a_{\text{H}^+}$), a nonprotonic function $p\text{O}^{2-}$ ($p\text{O}^{2-} = \log a_{\text{O}^{2-}}$) which is related to the acidity of the melt,⁹ can be defined for molten salts, $a_{\text{O}^{2-}}$ being the activity of the oxygen ion in the melt. Eq. [2] can then be written as

$$\phi_{\text{rev}} = \phi_{\text{rev}}^0 + \frac{2.3RT}{4F} \log P_{\text{O}_2} + \frac{2.3RT}{2F} p\text{O}^{2-} \quad [3]$$

where P_{O_2} is the pressure of oxygen. From this equation, it follows that both an increase in oxygen pressure and an increase in $p\text{O}^{2-}$ (melt becomes more acid) will increase the corrosion rate of a metal immersed in a molten salt by making the redox potential of the melt more noble. The effect of oxygen pressure on the corrosion rate is shown schematically in Fig. 8, assuming that $p\text{O}^{2-}$ remains constant. The solid line in Fig. 8 represents the potential dependence of the metal dissolution rate, while the dashed lines represent the potential dependence of the oxygen reduction rate. From the intersection of these two curves corrosion potential and corrosion current density (rate) can be determined. When the partial pressure of oxygen is increased from $P_{\text{O}_2}^1$ to $P_{\text{O}_2}^2$, the corrosion rate (in electrical units A/cm^2) increases from i_{corr}^1 to i_{corr}^2 , while the corrosion potential is shifted in the noble (positive) direction from ϕ_{corr}^1 to ϕ_{corr}^2 .

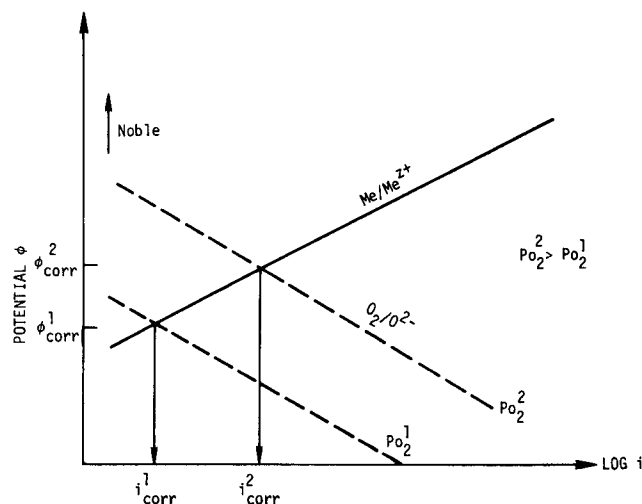


Fig. 8—Effect of oxygen pressure on corrosion rates in molten salts (schematic).

It should be noted here that the thermodynamic considerations can only predict trends of the reactions; the rate of the corrosion process will also depend on the kinetics of the reactions involved. An experimental verification of the theoretical curves in Fig. 8 can be found in the curves for Inconel 718 in Fig. 4, where lowering of the oxygen pressure by purging the quartz tube with nitrogen resulted in a shift of the whole polarization curve in the negative direction, as predicted in Fig. 8. Similar results were found for all other alloys studied.

The effect of water contamination has been treated from a thermodynamic standpoint by Edeleanu and Littlewood⁸ and Littlewood and Argent,¹⁰ who showed that for a given concentration of water, the redox potential of the melt is determined not by the activity of the water, but by the activity of its hydrolysis and dissociation products, H^+ , O^{2-} , H_2 , and O_2 , which in turn are fixed by equilibria with oxides and with partial pressure of gases in the atmosphere over the melt. It is, therefore, more difficult to make predictions concerning the effect of water. The damaging effect of moisture reported here was also observed by Gurovich¹¹ who concludes in a study of the action of fused chloride on nickel, copper, and certain steels that fresh and dehydrated salt should always be used for testing metals in salts as the presence of even traces of moisture in the salt appreciably increases corrosion losses. This conclusion was also reached by Stepanov and Kachina-Pullo¹² in a study of corrosion of steels and nickel in fused KCl and $MgCl_2$ at 800° and 850°C, who found $MgCl_2$ more aggressive due to its high water content. Littlewood and Argent,¹⁵ found for nickel in NaCl-KCl at 700°C under argon, that in the "undried" melt the potential of the nickel rose more rapidly than in the "dry" melt and that this indicated a more rapid rise in the nickel ion content of the melt.

The higher corrosion rates when a platinum crucible was used instead of a quartz crucible can be explained by galvanic action between the test specimen and the platinum crucible, the specimen being in electrical contact with the platinum. In the present experiment, the area of the platinum crucible (cathode) exposed to the melt was much larger than the area of the test specimen (anode). Due to this unfavorable anode/cathode area ratio, the dissolution rate of the anode is sharply increased, as has been recently discussed by Mansfeld.¹³ The increase of dissolution rates due to galvanic action, which is very common in aqueous corrosion, is explained in Fig. 9 where it is assumed that the only reaction on platinum is reduction of oxygen. Without coupling to platinum the corrosion current of the specimen would be I_{corr}^A and the corrosion potential would be ϕ_{corr}^A . When electrical contact is made, the dissolution current of the anode (test specimen) will increase from I_{corr}^A to I_a^A and will be equal to the cathodic current I_c^{Pt} on the platinum electrode and equal to the galvanic current I_g^A :

$$I_a^A = I_c^{Pt} = I_g^A \quad [4]$$

As a consequence the potential will increase from ϕ_{corr}^A to ϕ_g . The corrosion rates of all specimens have indeed been increased when experiments were carried out in platinum crucibles, although this increase was different for each alloy indicating different dissolution

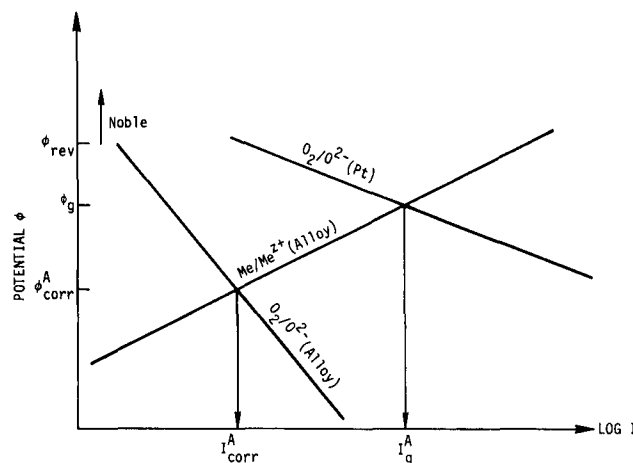


Fig. 9—Effect of galvanic coupling to a more noble metal on corrosion rates (schematic).

kinetics. These findings confirm the electromechanical character of corrosion of metals in fused salts reported by many investigators.

Effects of Alloy Composition

Our results in molten NaCl using quartz crucibles are similar to those reported by Stepanov and Kachina-Pullo¹² who concluded that in molten KCl, the effect of the composition of various Cr-Ni steels on the corrosion rate is not very great. Alloying components such as Ti, Nb, or Mo had virtually no effect; the presence of tungsten, however, reduced the corrosion resistance of steel.^{12,14} In the present study, it was also observed that Haynes 188 containing 14 pct W had a higher corrosion rate than the other superalloys or nickel, Table I. Corrosion rates in Table I are comparable to results for Ni-Cr steels obtained by these workers in short time (<10 h) experiments, average values in KCl being 380 mdd for 800°C and 550 mdd for 850°C, indicating similar corrosion behavior of Ni-Cr steels and superalloys.

Moskowitz and Redmerski⁷ also found that all superalloys tested in molten KCl or LiF were seriously corroded in the presence of air. These authors did not measure corrosion rates; in a general ranking of the alloys based on creep-rupture tests, Haynes 25 containing about 15 pct W and Rene' 41 showed better performance than Inconel 702 and Inconel X for both uncoated and salt-coated materials, which is contrary to present results.

Composition of Corrosion Products

There is good agreement between the analysis of the insoluble corrosion products by mass spectroscopy and structural analysis by X-ray diffraction. For Inconel 718, for example, the former results indicate strong preferential dissolution of chromium and to a lesser extent of iron, while much less nickel is found than in the bulk. The corrosion products were identified as Cr_2O_3 and Fe_3O_4 or $NiFe_2O_4$. Similar agreement was found for other alloys. Moskowitz and Redmerski⁷ also analyzed corrosion products from superalloys by spectroscopy and X-ray diffraction. Chromium and nickel

(also cobalt for Haynes 25) were found by spectroscopy as major constituents with other elements presently related to alloy composition. NiO, spinels, and Fe₂O₃-type oxides were found for Inconel 702, Inconel X and Rene' 41, CoO · 3NiO, spinels and Co₃O₄ were found for Haynes by X-ray diffraction. The preferential dissolution of tungsten found by Haynes 188 in the present investigation, Table II, consistent with the occurrence of CoWo₄ as major corrosion product was not reported in Ref. 7 which might reflect a superior corrosion behavior of Haynes 25 as compared to Haynes 188. The Russian workers^{12,14} found by chemical analysis that the corrosion products on Cr-Ni steels consisted mainly of chromium oxides, a small amount of iron oxide, and an even smaller amount of nickel oxides.

Analysis of the soluble corrosion products, Table III, showed that these consisted mainly of nickel and cobalt, again in agreement with Stepanov and Kachina-Pullo,¹² who found that far less chromium than nickel is transferred to the fused system irrespective of the initial content of these components in the steels. Only small amounts of soluble chromium corrosion product (chromate) were found similar to the results of Moskowitz and Redmerski,⁷ who assume that these chromates are formed in a reaction involving chromium or chromium oxide, salt, and oxygen.

The presence of the molten salt leads to formation of oxides and spinels which are not protective as indicated by the high corrosion rates and the absence of passivity as suggested by the shape of the polarization curves.

CONCLUSIONS

1) Corrosion rates of superalloys in molten NaCl at 820°C are highly dependent on oxygen pressure and to some extent on the water content of the melt.

2) The alloy composition does not influence corrosion rates very much. It was found, however, in agreement with work on Ni-Cr steels in molten KCl¹² that tungsten has an adverse effect.

3) The high dissolution rates and the shape of the polarization curves indicate that the oxides formed in molten NaCl are not protective.

4) Analysis of sodium content in the alloy after exposure to molten NaCl indicates diffusion of Na into the bulk of the metal which might be the reason for the degradation of mechanical properties.

ACKNOWLEDGMENT

The authors acknowledge discussions with Dr. L. E. Topol concerning thermodynamics in molten salts, and experimental support by R. A. Meyer and J. H. Davis (mass spectroscopy), C. Rhodes (X-ray analysis), and D. Hengstenberg (atomic absorption spectroscopy).

REFERENCES

1. N. E. Paton, W. M. Robertson, and F. Mansfeld: *Met. Trans.*, 1973, vol. 4, pp. 317-20.
2. A. Rahmel: *Werks. Korros.*, 1969, vol. 19, p. 750.
3. G. Baudo, A. Tamba, and G. Bombara: *Corros.*, 1970, vol. 26, p. 193.
4. G. J. Janz and A. Conte: *Electrochim. Acta*, 1964, vol. 9, p. 1279.
5. V. N. Devyatkin and E. A. Ukshe: *J. Appl. Chem. USSR*, 1962, vol. 35, p. 1276.
6. G. Danner and M. Rey: *Electrochim. Acta*, 1961, vol. 4, p. 274.
7. A. Moskowitz and L. Redmerski: *Corros.*, 1961, vol. 17, p. 305t.
8. C. Edeleanu and R. Littlewood: *Electrochim. Acta*, 1960, vol. 3, p. 195.
9. H. Lux: *Z. Elektrochem.*, 1939, vol. 45, p. 303.
10. R. Littlewood and E. J. Argent: *Electrochim. Acta*, 1961, vol. 4, p. 114.
11. E. I. Gurovich: *J. Appl. Chem. USSR*, 1954, vol. 27, p. 395.
12. S. I. Stepanov and E. B. Kachina-Pullo: *Zh. Prikl. Khim.*, 1964, vol. 37, p. 379.
13. F. Mansfeld: *Corros.*, 1971, vol. 27, p. 436.
14. S. I. Stepanov and E. B. Kachina-Pullo: *Zh. Prikl. Khim.*, 1962, vol. 35, p. 1328.
15. R. Littlewood and E. J. Argent: *Electrochim. Acta*, 1961, vol. 4, p. 155.